ORGANOMETALLICS

pubs.acs.org/Organometallics Article

Evaluating Electron Transfer Reactivity of Rare-Earth Metal(II) Complexes Using EPR Spectroscopy

Samuel A. Moehring and William J. Evans*



Cite This: Organometallics 2020, 39, 1187-1194



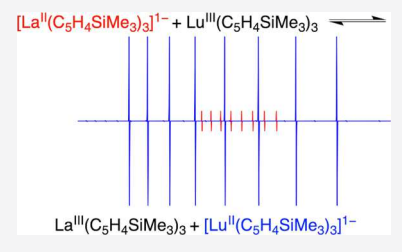
ACCESS

III Metrics & More

Article Recommendations

Supporting Information

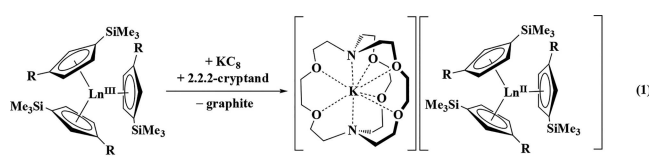
ABSTRACT: To evaluate the relative reducing capacities of rare-earth metal complexes of Sc(II), Y(II), and complexes of the lanthanide metals in their +2 oxidation state, a series of reactions of trivalent $\operatorname{Ln^{III}}A_3$ compounds with divalent $[\operatorname{Ln'^{II}}A'_3]^{1-}$ complexes has been examined, where $\operatorname{Ln} = \operatorname{Sc}$, Y, or a lanthanide and A is $\operatorname{C}_5H_4\operatorname{SiMe_3}$ ($\operatorname{Cp'}$), $\operatorname{C}_5H_3(\operatorname{SiMe_3})_2$ ($\operatorname{Cp''}$), $\operatorname{C}_5\operatorname{Me_4H}$ ($\operatorname{Cp^{tet}}$), $\operatorname{N}(\operatorname{SiMe_3})_2$ (NR_2), 2,6- ${}^t\operatorname{Bu_2}$ -C₆H₃O (OAr), or 2,6- ${}^t\operatorname{Bu_2}$ -4-Me-C₆H₂O ($\operatorname{OAr'}$). The specific combinations were chosen to allow evaluation by EPR spectroscopy of the $\operatorname{Ln}(\operatorname{II})$ complex. The $[\operatorname{Ln^{II}}\operatorname{Cp'_3}]^{1-}$ complexes of Y(II), $\operatorname{La}(\operatorname{II})$, and $\operatorname{Lu}(\operatorname{II})$ have similar reducing abilities in that they all reduce $\operatorname{Ln^{III}}\operatorname{Cp'_3}$ complexes of the other metals in this group. However, these Y(II), $\operatorname{La}(\operatorname{II})$, and $\operatorname{Lu}(\operatorname{II})$ complexes all are stronger reductants



than $[Gd^{II}Cp'_3]^{1-}$, which cannot reduce $Ln^{III}Cp'_3$ complexes of Y, La, and Lu. These results do not apply to all ligand sets, since $[Gd^{II}(NR_2)_3]^{1-}$ can reduce $Y^{III}(NR_2)_3$ to $[Y^{II}(NR_2)_3]^{1-}$. The amide and aryloxide complexes of Y and Sc are similar in that $[Y^{II}(NR_2)_3]^{1-}$ reduces $Sc^{III}(NR_2)_3$ and $[Y^{II}(OAr')_3]^{1-}$ reduces $Sc^{III}(NR_2)_3^{1-}$ and $[Y^{II}(OAr')_3]^{1-}$ reduce $Y^{III}Cp'_3$. Both $[Y^{II}(NR_2)_3]^{1-}$ and $[Y^{II}(OAr')_3]^{1-}$ reduce $Y^{III}Cp'_3$. La $[La^{II}Cp^{te}_3]^{1-}$ has reductive capacity similar to that of $[La^{II}Cp'_3]^{1-}$, and both are stronger reductants than $[La^{II}Cp''_3]^{1-}$. None of the $Ln^{II}I_2$ complexes of Sm, Tm, Dy, and Nd can reduce $Ln^{III}A_3$ complexes of Y and La to $[Ln^{II}A_3]^{1-}$. In the "same-metal-different-ligands" reactions, multiple EPR signals are found, suggesting that ligand exchange occurs alongside the electron transfer reactivity.

■ INTRODUCTION

Redox chemistry is one of the two most fundamental types of reactivity, along with acid-base chemistry. Inherent in the utilization of redox reactions is the availability of different oxidation states and the redox potentials that interconnect them. In the field of lanthanide chemistry, new opportunities have arisen with the discovery that stable molecular complexes of +2 ions could be isolated not only for Eu, Yb, Sm, Tm, Dy, and Nd, but also for all the rest of the lanthanides except radioactive Pm. 1-6 Examples with silylcyclopentadienyl ligands are shown in eq 1. Surprisingly, these new Ln(II) ions made by reduction of 4f" Ln(III) ions had properties consistent with 4f"5d1 electron configurations rather than the $4f^{n+1}$ configurations of Eu(II), Yb(II), Sm(II), Tm(II), Dy(II), and Nd(II). 7,8 Although these recently discovered +2 oxidation states are being found in an increasing number of coordination environments, 9-16 information on the redox potentials of these ions has been elusive. The highly reducing species can react with supporting electrolytes and in some cases with THF solvent. For example, reduction of $Ln^{III}Cp^{Me}_{3}$ ($Cp^{Me} = C_5H_4Me$; Ln = La, Pr) according to eq 1, presumably to form [LnIICpMe3]1- complexes, causes ring opening of THF to form products containing $[O(CH_2)_4]^{2-}$ dianions.¹⁷ Since the new Ln(II) complexes can be generated with K and Na (eq 1), the redox potentials must be less negative than -2.7 V vs SHE. ¹⁸ However, the relative reactivities of these species and the dependence of their redox potentials on the specific metal and the ligand remain unknown.



R = H; Ln = Y, La, Ce, Pr, Gd, Tb, Ho, Er, Lu R = SiMe₃; Ln = La, Ce, Pr, Nd

To fill this gap in experimental data, Ln^{III}A₃ complexes that are known to form new Ln(II) ions (A = anion such as cyclopentadienyl, amide, or aryloxide) were reacted with [Ln^{II}A₃]¹⁻ complexes involving either different metals or different ligands to evaluate their comparative reduction chemistry. To accomplish this comparison, Ln(II) systems were selected that allow EPR spectroscopy to be used to interrogate the systems. This is most readily accomplished with La, Gd, Lu, Y, and Sc.^{2,4-6,19} It was found that EPR spectroscopy even allows characterization when complicated mixtures of products are formed. The comparative reaction data are presented along with a discussion of the implications for rareearth reduction chemistry.

Received: December 9, 2019 Published: March 23, 2020





RESULTS

Methods. Each reaction described below involves reaction of a THF solution of a [LnIIA3]1- complex with a THF solution of Ln^{III}A₃, where either the metal or ligand of the Ln(III) reagent differs from that of the Ln(II) reagent. Some of the [Ln^{II}A₃]¹⁻ complexes utilized in this study were too reactive to be isolated and were identified only through EPR spectroscopy. In order to maintain a consistent experimental approach for both isolable and nonisolable compounds, the "reductant" [Ln^{II}A₃]¹⁻ species was generated by passing a THF solution (~10 mg/mL; 10-20 mM) of Ln^{III}A₃ through a pipet packed with KC₈ that had been chilled to −35 °C. The resulting intensely colored solution was dripped onto a THF solution (10-20 mM, equimolar with the "reductant" species) of a "substrate" LnIIIA3 compound (where Ln or A was different) containing 1 equiv of 2.2.2-cryptand (crypt). In each case, the mixture was then loaded into a chilled EPR tube and quickly frozen. This method allowed the unstable Ln(II) compounds to be quickly generated and trapped in the frozen solution. The whole process took no longer than 90 s. Crypt was included to stabilize any Ln(II) products generated, since it has been seen in this study and in others⁴ that thermal stability of Ln(II) complexes can be enhanced by the presence of crypt. Crypt could not be included in the reductant solution, however, because passing a THF solution of only crypt through KC₈ produces a deep-blue solution of an electride species that can act as a reductant itself (Figure S42).^{20,21}

The reactions with DyI₂ and NdI₂ were carried out with slight modifications of the procedure. Soluble DyI₂(THF)₅ and NdI₂(THF)₅ were first extracted from base-free DyI₂ and NdI₂ with THF at $-35\,^{\circ}\text{C}$. These solutions were then reacted with the substrate Ln(III) compounds under the same conditions as in the other experiments, i.e., at $-35\,^{\circ}\text{C}$ in THF. Since DyI₂(THF)₅ and NdI₂(THF)₅ are known to decompose in THF over hours at room temperature, 22 the reactions were done quickly while the colors indicative of DyI₂(THF)₅ and NdI₂(THF)₅ were still present.

Reduction of a Ln'^{III}A'₃ "substrate" by a [Ln^{II}A₃]¹⁻ "reductant" (where Ln and Ln' are the two metals and A and A' are the ligands involved in the electron transfer experiment) was counted as a successful reaction only when the [Ln'^{II}A'₃]¹⁻ species could be detected by EPR spectroscopy, i.e., loss of the EPR signal of the [Ln^{II}A₃]¹⁻ reactant was not sufficient. The reactions in this paper are written to show when a transformation occurred in the forward direction. Since equilibrium constants for these systems are not known, only reactions in the forward direction are reported. All of the EPR spectra used for this study can be found in the Supporting Information.

Overview. The logic of the order of presentation of the following sections is described here. Since the $(Cp'_3)^{3-}$ ligand set $(Cp' = C_5H_4SiMe_3)$ is known to stabilize all of the Ln(II) ions except small Sc(II) and radioactive Pm(II),⁴ this ligand set was chosen for the initial investigations in which the ligand set was kept constant and the metal was varied. Metal variation was next studied with complexes of the $[(NR_2)_3]^{3-}$ ligand set $(R = SiMe_3)$ since several are available and this provides a comparison of the ligand sets $(Cp'_3)^{3-}$ versus $[(NR_2)_3]^{3-}$. Ligand variation is subsequently described with yttrium as the sole metal since a wide variety of Y(II) compounds have been identified by EPR spectroscopy. After the yttrium section is a section discussing only scandium complexes for a comparison of Y versus Sc. La chemistry is then described last, since it shows the most ligand exchange. Ligand exchange is then discussed with a final section

on reduction with traditional Ln(II) ions of Sm, Tm, Dy, and Nd.

Reactions of $[Ln^{II}Cp'_3]^{1-}$ with $Ln'^{III}Cp'_3$ ($Cp'^{1-} = C_5H_4SiMe_3^{1-}$). Treatment of colorless $La^{III}Cp'_3(THF)$ ($La^{III}: 4f^0Sd^0$, S=0) with maroon $[Y^{II}Cp'_3]^{1-}$ (⁸⁹Y^{II}: $S=^1/_2$, $I=^1/_2$, 100% abundance) in THF (reaction 2) gave a maroon mixture with an EPR spectrum containing signals for both $[La^{II}Cp'_3]^{1-}$ (¹³⁹ $La^{II}: 4f^0Sd^1$, $S=^1/_2$, $I=^7/_2$, 99.9% abundance) and $[Y^{II}Cp'_3]^{1-}$ (Figure 1).^{2,4} Hence, Y(II) reduced La(III), but the

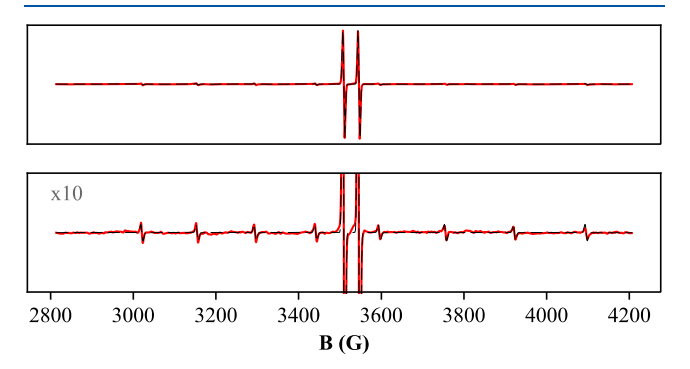


Figure 1. Room-temperature X-band EPR spectrum (red solid) and simulated spectrum (black dashed) of the products of reaction 2 in the forward direction at (top) $\times 1$ and (bottom) $\times 10$. Signals are present at g = 1.99, $A(^{89}Y) = 37.1$ G ($[Y^{II}Cp'_{3}]^{1-}$) and g = 1.97, $A(^{139}La) = 153.4$ G ($[La^{II}Cp'_{3}]^{1-}$).

reaction did not form La(II) exclusively. Consistent with this, treatment of yellow $Y^{III}Cp'_3$ (Y^{III} : $4d^0$, S=0) with maroon [La^{II}Cp'₃]¹⁻ formed [Y^{II}Cp'₃]¹⁻, i.e., La(II) can reduce Y(III). These results (reaction 2) indicate that the reduction potentials of La^{III}Cp'₃(THF) and $Y^{III}Cp'_3$ are very similar.

$$[Y^{II}Cp'_{3}]^{1-} + La^{III}Cp'_{3}(THF) \rightleftharpoons Y^{III}Cp'_{3} + [La^{II}Cp'_{3}]^{1-}$$
(2)

The four combinations of Ln(II) reagents of Y and Lu with Ln'(III) substrates of La and Lu gave similar results (reactions 3 and 4; Figure 2). Hence, La^{III}Cp'_3(THF), Y^{III}Cp'_3, and Lu^{III}Cp'_3 (Lu^{III}: 4f^{14}, S=0) all have similar reduction potentials. This was somewhat surprising since the half-lives of the complexes (measured by UV–vis spectroscopy) are quite different: $[K(crypt)][Lu^{II}Cp'_3]$ (175Lu^{II}: 4f¹⁴5d¹, S=1/2, I=1/2).

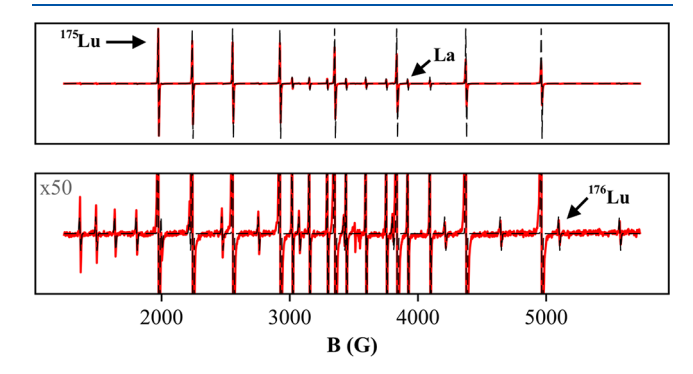


Figure 2. Room-temperature X-band EPR spectrum (red solid) and simulated spectrum (black dashed) of the products of reaction 4 in the reverse direction at (top) ×1 and (bottom) ×50. Signals are present at g=1.97, $A(^{139}\text{La})=153.5$ G ($[\text{La}^{\text{II}}\text{Cp'}_3]^{1-}$); g=1.97, $A(^{176}\text{Lu})=425.3$ G ($[^{175}\text{Lu}^{\text{II}}\text{Cp'}_3]^{1-}$); and g=1.97, $A(^{176}\text{Lu})=300.3$ G ($[^{176}\text{Lu}^{\text{II}}\text{Cp'}_3]^{1-}$). The large Lu hyperfine coupling, which is not first-order, has been discussed previously.⁴

 $^{7}/_{2}$, 97.4% abundance; $^{176}\text{Lu}^{II}$: $4f^{14}5d^{1}$, $S = ^{1}/_{2}$, I = 7, 2.6% abundance) has a first-order $t_{1/2}$ of 19 min, 4 and [K(crypt)]-[Y^{II}Cp'₃] has a second-order $t_{1/2}$ of 2.3 h at 3 mM, while [K(crypt)][La^{II}Cp'₃] appears to have a half-life of over 30 h.

$$[Lu^{II}Cp'_{3}]^{1-} + Y^{III}Cp'_{3} \rightleftharpoons Lu^{III}Cp'_{3} + [Y^{II}Cp'_{3}]^{1-}$$
 (3)

$$[Lu^{II}Cp'_{3}]^{1-} + La^{III}Cp'_{3}(THF) \rightleftharpoons Lu^{III}Cp'_{3} + [La^{II}Cp'_{3}]^{1-}$$
 (4)

In contrast to these reactions that proceed from either direction, $[Gd^{II}Cp'_3]^{1-}$ $(Gd^{II}: 4f^75d^1, S = 4; ^{155}Gd, I = ^3/_2, 14.8\%; ^{157}Gd, I = ^3/_2, 15.6\%; hyperfine splitting is not observed in the EPR spectrum of <math>[Gd^{II}Cp'_3]^{1-}$) does not reduce $La^{III}Cp'_3(THF)$, $Y^{III}Cp'_3$, or $Lu^{III}Cp'_3$. Consistent with this, $Gd^{III}Cp'_3$ $(Gd^{III}: 4f^7, S = ^7/_2)$ is reduced by $[La^{II}Cp'_3]^{1-}$, $[Y^{II}Cp'_3]^{1-}$, and $[Lu^{II}Cp'_3]^{1-}$ (reactions 5–7). It is not obvious why this was the case. The second-order $t_{1/2}$ of $[Gd^{II}Cp'_3]^{1-}$ at 3 mM is 89 h.

$$[Y^{II}Cp'_{3}]^{1-} + Gd^{III}Cp'_{3} \rightarrow Y^{III}Cp'_{3} + [Gd^{II}Cp'_{3}]^{1-}$$
 (5)

$$[La^{II}Cp'_{3}]^{1-} + Gd^{III}Cp'_{3} \rightarrow La^{III}Cp'_{3}(THF) + [Gd^{II}Cp'_{3}]^{1-}$$
(6)

$$[Lu^{II}Cp'_{3}]^{1-} + Gd^{III}Cp'_{3} \rightarrow Lu^{III}Cp'_{3} + [Gd^{II}Cp'_{3}]^{1-}$$
(7)

The $4f^8Sd^1$ Tb(II) complex $[Tb^{II}Cp'_3]^{1-}$ ($^{159}Tb^{II}$: $4f^8Sd^1$, $S = ^{7}/_2$, $I = ^{3}/_2$, 100% abundance) was also studied as a reductant since it has an electron configuration close to that of $4f^7Sd^1$ Gd(II) in $[Gd^{II}Cp'_3]^{1-}$. Tb $^{III}Cp'_3$ (Tb^{III} : $4f^8$, S = 3) was not used as a substrate since the anticipated $[Tb^{II}Cp'_3]^{1-}$ product would not be identifiable by X-band EPR spectroscopy at either 77 K or room temperature. Thus, only reactions in which $[Tb^{II}Cp'_3]^{1-}$ acted as a reducing agent were examined. $[Tb^{II}Cp'_3]^{1-}$ reduces all of the substrates that are unreactive with $[Gd^{II}Cp'_3]^{1-}$, namely, $La^{III}Cp'_3$ (THF), $Y^{III}Cp'_3$, and $Lu^{III}Cp'_3$, as well as $Gd^{III}Cp'_3$ (reactions 8-11). This gives a ranking of these $[Ln^{II}Cp'_3]^{1-}$ complexes, from most reducing to least reducing, as $Tb(II) \gtrsim Y(II) \approx La(II) \approx Lu(II) > Gd(II)$. Tb(II) could be more reducing than Y(II), La(II), and Lu(II), but it is not known whether these three ions would be able to reduce Tb(III) to Tb(II) in this ligand set.

$$[Tb^{II}Cp'_{3}]^{1-} + Y^{III}Cp'_{3} \rightarrow Tb^{III}Cp'_{3} + [Y^{II}Cp'_{3}]^{1-}$$
 (8)

$$[Tb^{II}Cp'_{3}]^{1-} + La^{III}Cp'_{3}(THF) \rightarrow Tb^{III}Cp'_{3} + [La^{II}Cp'_{3}]^{1-}$$
 (9)

$$[Tb^{II}Cp'_{3}]^{I-} + Lu^{III}Cp'_{3} \rightarrow Tb^{III}Cp'_{3} + [Lu^{II}Cp'_{3}]^{I-} \eqno(10)$$

$$[Tb^{II}Cp'_{3}]^{1-} + Gd^{III}Cp'_{3} \rightarrow Tb^{III}Cp'_{3} + [Gd^{II}Cp'_{3}]^{1-}$$
(11)

Reactions of $[Ln^{II}(NR_2)_3]^{1-}$ with $Ln'^{III}(NR_2)_3$ Complexes $(R = SiMe_3)$. The $[(NR_2)_3]^{3-}$ ligand set $(R = SiMe_3)$ is known to allow the isolation of complexes of Ln(II) ions for Sc, Y, Nd, Gd, Tb, Ho, and Er as well as the traditional divalent ions of Eu, Yb, Sm, and $Tm.^{6,9,12,23-25}$ Reactions of amide complexes were studied to determine whether the trend in the reducing abilities of the metals that was established with Cp' would change with different ligands. For these studies, only $[Y^{II}(NR_2)_3]^{1-}$ and

 $[Sc^{II}(NR_2)_3]^{1-}$ (45Sc^{II}: 3d¹, $S = {}^1/_2$; $I = {}^7/_2$, 100% abundance) can be used to detect successful reductions, as they are the only Ln(II) compounds in this ligand set with known EPR spectra at 77 K and room temperature. 6,26

While $[Y^{II}(NR_2)_3]^{1-}$ can reduce $Sc^{III}(NR_2)_3$ ($Sc^{III}: 3d^0, S = 0$) to $[Sc^{II}(NR_2)_3]^{1-}$ (reaction 12), the reverse reaction (reaction 13) does not occur (Figure 3), as no signals consistent with

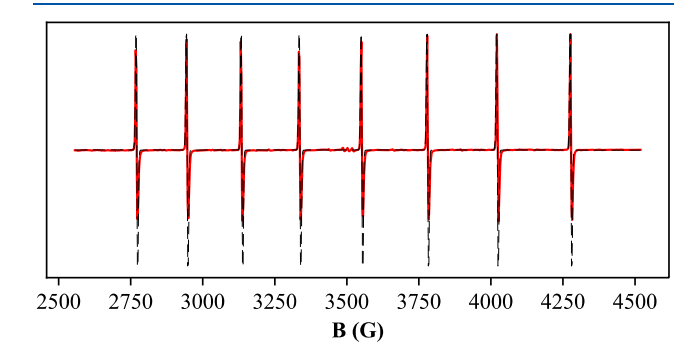


Figure 3. Room-temperature X-band EPR spectrum (red solid) and simulated spectrum (black dashed) of the products of reaction 13. A signal is present at g = 1.98, $A(^{45}Sc) = 214.9$ G ([Sc^{II}(NR₂)₃]¹⁻).

 $[Y^{II}(NR_2)_3]^{1-}$ (g = 1.97, $A(^{89}Y) = 110.5$ G) are observed. Therefore, $[Y^{II}(NR_2)_3]^{1-}$ is a stronger reductant than $[Sc^{II}(NR_2)_3]^{1-}$.

$$[Y^{II}(NR_2)_3]^{1-} + Sc^{III}(NR_2)_3 \rightarrow Y^{III}(NR_2)_3 + [Sc^{II}(NR_2)_3]^{1-}$$
 (12)

$$[Sc^{II}(NR_2)_3]^{1-} + Y^{III}(NR_2)_3 \rightarrow Sc^{III}(NR_2)_3 + [Y^{II}(NR_2)_3]^{1-}$$
 (13)

Both $[Gd^{II}(NR_2)_3]^{1-}$ and $[Tb^{II}(NR_2)_3]^{1-}$ can reduce the Y(III) and Sc(III) compounds (reaction 14 and Figure S20), so these two compounds are either as reducing or more reducing than $[Y^{II}(NR_2)_3]^{1-}$. This leads to the following ranking of these $[Ln^{II}(NR_2)_3]^{1-}$ complexes from most reducing to least reducing: $Tb(II) \approx Gd(II) \gtrsim Y(II) > Sc(II)$. The Gd(II) versus Y(II) results with the $[(NR_2)_3]^{3-}$ ligand set, where Gd(II) is comparable to Y(II), are opposite to those with the $(Cp'_3)^{3-}$ ligand set, where Y(II) is a stronger reductant than Gd(II). This indicates that the order of the reducing abilities of the new Ln(II) ions is not the same in every ligand environment. To investigate this hypothesis further, experiments comparing the same Ln(II) in different ligand sets were carried out.

$$[Gd^{II}(NR_2)_3]^{1-} + Y^{III}(NR_2)_3 \rightarrow Gd^{III}(NR_2)_3 + [Y^{II}(NR_2)_3]^{1-}$$
 (14)

Reactions of $[Y^{II}A_3]^{1-}$ with $Y^{III}A'_3$ Complexes (A, A' = Anion). The investigation of different ligand sets on the same metal was initially conducted with yttrium as the metal since a wide variety of Y(II) compounds have been identified by EPR spectroscopy. The Y(II) compounds investigated display a range of hyperfine coupling constants: $[Y^{II}Cp'_3]^{1-}$, $A(^{89}Y) = 36.6 \text{ G}_5^2$ $[Y^{II}(NR_2)_3]^{1-}$, $A(^{89}Y) = 110 \text{ G}_5^{26}$ and " $[Y^{II}(OAr)_3]^{1-}$ ", $A(^{89}Y) = 156 \text{ G}$ (OAr = 2,6- t Bu₂C₆H₃O). Is the should be noted that the aryloxide complex has not been characterized by X-ray crystallography. Since the A value has been shown to increase with the amount of metal contribution to the singly occupied molecular orbital (SOMO), It was hypothesized that a higher

A value (i.e., more metal character in the SOMO) might increase the reducing power of the resulting Y(II) compound.

 $[Y^{II}Cp'_3]^{1-}$ is the weakest reductant of the compounds studied with yttrium, as it cannot reduce any of the other Y(III) compounds (reactions 15 and 16). Consistent with this, $Y^{III}Cp'_3$ can be reduced by all of the other Y(II) species (reactions 17 and 18). $[Y^{II}(NR_2)_3]^{1-}$ reduces $Y^{III}(OAr)_3$ to $[Y^{II}(OAr)_3]^{1-}$ (reaction 19), but the reverse reaction occurs as well (reaction 20). Therefore, the ordering of ligand sets, in terms of the reducing ability they confer on Y(II) compounds, is $(OAr)_3^{3-} \approx [(NR_2)_3]^{3-} > (Cp')_3^{3-}$.

$$[Y^{II}Cp'_{3}]^{1-} + Y^{III}(OAr)_{3} \rightarrow unknown EPR-active species$$
 (15)

$$[Y^{II}Cp'_{3}]^{1-} + Y^{III}(NR_{2})_{3} \rightarrow Y^{III}Cp'_{3} + [Y^{II}(NR_{2})_{3}]^{1-}$$
(16)

$$\begin{split} &[Y^{II}(OAr)_3]^{l-} + Y^{III}C{p'}_3 \rightarrow Y^{III}(OAr)_3 + [Y^{II}C{p'}_3]^{l-} \\ &+ \text{ other EPR-active species} \end{split} \tag{17}$$

$$[Y^{II}(NR_2)_3]^{1-} + Y^{III}Cp'_3 \rightarrow Y^{III}(NR_2)_3 + [Y^{II}Cp'_3]^{1-}$$
(18)

$$\begin{split} & [Y^{II}(NR_2)_3]^{1-} + Y^{III}(OAr)_3 \rightarrow Y^{III}(NR_2)_3 \\ & + [Y^{II}(OAr)_3]^{1-} + \text{other EPR-active species} \end{split} \tag{19}$$

$$[Y^{II}(OAr)_3]^{1-} + Y^{III}(NR_2)_3 \rightarrow [Y^{II}(NR_2)_3]^{1-} + Y^{III}$$

$$(OAr)_3 \qquad (20)$$

Some of these yttrium reactions led to additional EPR signals that cannot be attributed to known Y(II) compounds. For example, the room-temperature EPR spectrum of reaction 15 (Figure 4) contains a variety of signals attributable to Y(II)

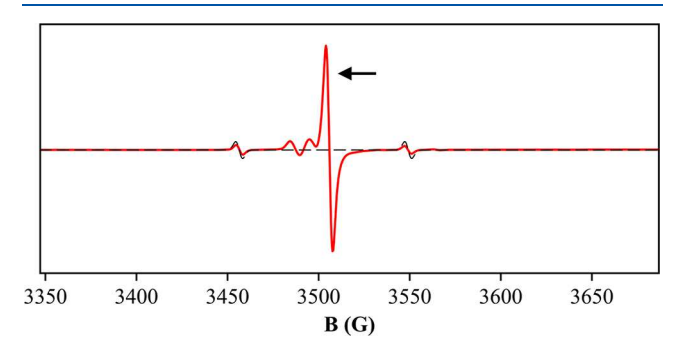


Figure 4. Room-temperature X-band EPR spectrum (red solid) and simulated spectrum (black dashed) of the products of reaction 15. Signals are present at g = 2.00 (likely electride, labeled with a black arrow) and g = 2.00, A = 92.8 G (the highest A value that could be simulated for these data, an unknown Y(II) species).

complexes (by their doublet pattern), but none that can be assigned to known Y(II) compounds (the large central single line at g=2.00 probably arises from electride 14,20,21 in the sample). The appearance of multiple Ln(II) species was observed in experiments with other metals (vide infra) and will be described in more detail in those sections.

Reactions of $[Sc^{II}A_3]^{1-}$ with $Sc^{III}A'_3$ Complexes. Comparison of different ligands on the same metal was also carried out with the Sc(II) complexes $[Sc^{II}(NR_2)_3]^{1-}$ (A = 214 G) and $[Sc^{II}(OAr')_3]^{1-}$ (OAr' = 2,6- tBu_2 -4-Me-C₆H₂O) (A = 1

291 G). 6,13 The Sc(II) amide and aryloxide mutually reduce one another, i.e., $[Sc^{II}(NR_2)_3]^{1-}$ reduces $Sc^{III}(OAr')_3$ and $[Sc^{II}(OAr')_3]^{1-}$ reduces $Sc^{III}(NR_2)_3$ (reaction 21). A similar situation was observed with yttrium and these ligand sets.

$$[Sc^{II}(OAr')_3]^{1-} + Sc^{III}(NR_2)_3 \rightleftharpoons [Sc^{II}(NR_2)_3]^{1-} + Sc^{III}(OAr')_3$$
 (21)

Reactions of [La^{II}A₃]¹⁻ with La^{III}A'₃ Complexes. La(II) compounds were also investigated with different ligands since several options are known: [La^{II}Cp"₃]¹⁻ (Cp" = C₅H₃(SiMe₃)₂) ($A(^{139}La) = 133.5 \text{ G}$), [La^{II}Cp'₃]¹⁻ ($A(^{139}La) = 154 \text{ G}$), and [La^{II}Cptet₃]¹⁻ (Cp^{tet} = C₅Me₄H) ($A(^{139}La) = 291 \text{ G}$). La^{II}Cptet₃]¹⁻ can reduce La^{III}Cp'₃(THF) (reaction 22), and [La^{II}Cp'₃]¹⁻ can do the reverse reaction to reduce La^{III}Cptet₃ (reaction 23). [La^{II}Cptet₃]¹⁻ can also reduce La^{III}Cptet₃ or La^{III}Cp'₃(THF). [La^{II}Cp'₃]¹⁻ can also reduce La^{III}Cptet₃ or La^{III}Cp'₃(THF). [La^{II}Cp'₃]¹⁻ cannot reduce either La^{III}Cptet₃ or La^{III}Cp'₃(THF). [La^{II}Cp'₃]¹⁻ cannot reduce La^{III}Cp'₃(THF). Thus, the ordering of reducing strengths for ligand sets with La(II), from most reducing to least reducing, is $(Cp^{tet})_3^{3-} \approx (Cp')_3^{3-} > (Cp'')_3^{3-}$.

$$\begin{split} [La^{II}Cp^{tet}_{3}]^{1-} + La^{III}Cp'_{3}(THF) \rightarrow \\ La^{III}Cp^{tet}_{3} + [La^{II}Cp'_{3}]^{1-} + \textbf{La-A} + \textbf{La-B} \end{split} \tag{22}$$

$$\begin{split} & [La^{II}Cp'_{\,3}]^{1-} + La^{III}Cp^{tet}_{\ 3} \rightarrow La^{III}Cp'_{\,3}(THF) \\ & + [La^{II}Cp^{tet}_{\ 3}]^{1-} + \textbf{La-A} + \textbf{La-B} \end{split} \tag{23}$$

$$\begin{split} [La^{II}Cp^{tet}_{3}]^{1-} + La^{III}Cp''_{3} &\rightarrow La^{III}Cp^{tet}_{3} + [La^{II}Cp''_{3}]^{1-} \\ + \text{ other La(II) species} \end{split} \tag{24}$$

$$[La^{II}Cp'_{3}]^{1-} + La^{III}Cp''_{3} \rightarrow La^{III}Cp'_{3}(THF)$$

+ $[La^{II}Cp''_{3}]^{1-} + La-C + La-D$ (25)

In all of the above reactions with lanthanum, multiple species were present. This was previously observed for the reactions of yttrium complexes (vide supra) but not in the case of scandium, as no unidentified EPR signals were found in the Sc spectra. The EPR spectrum of reaction 22 contains signals for [La^{II}Cp'₃]¹⁻ (g = 1.97, $A(^{139}La)$ = 153.4 G) and two other unknown La(II) species labeled as La-A with $g_A = 1.96$, $A_A(^{139}La) = 186.5$ G and La-B with $g_B = 1.96$, $A_B(^{139}La) = 229.8$ G (Figure 5) and assigned as La(II) complexes on the basis of the eight-line patterns. The EPR spectrum of reaction 23 (the reverse of reaction 22) contains signals for $[La^{II}Cp'_3]^{1-}$ ($g = 1.97, A(^{139}La)$ = 153.5 G), $[La^{II}Cp^{tet}_3]^{1-}$ ($g = 1.95, A(^{139}La)$ = 290.0 G), and La-A and La-B (Figure 6). Multiple signals were also seen for reaction 25. The EPR spectrum from reaction 25 contains signals for its target compound $[La^{II}Cp''_3]^{1-}$ ($g = 1.96, A(^{139}La)$ = 133.6 G) as well as two unknown La(II) species labeled as La-**C** with $g_C = 1.96$, $A_C(^{139}\text{La}) = 144.8$ G and $\hat{\textbf{La}}$ -**D** with $g_D = 1.96$, $A_D(^{139}\text{La}) = 149.8 \text{ G.}$ Treatment of $La^{III}Cp'_3(THF)$ with [La^{II}Cp"₃]¹⁻, which does not result in the formation of the target compound [La^{II}Cp'₃]¹⁻, still contains the same two unknown La(II) species as reaction 25, i.e., La-C and La-D.

The EPR parameters from these reactions are listed in Table 1. The La(II) species observed here with A values differing from those of known compounds could be heteroleptic La(II) compounds formed by ligand exchange in the course of the

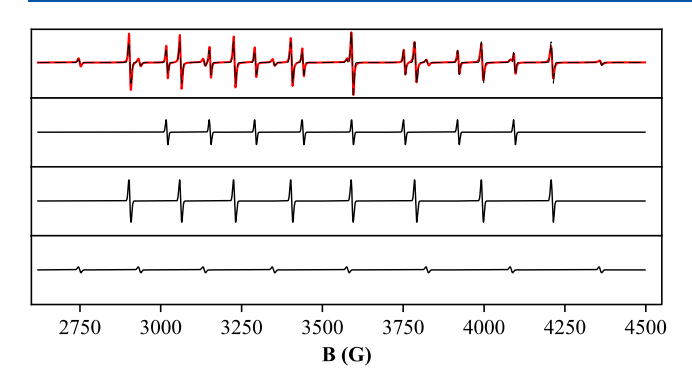


Figure 5. Room-temperature X-band EPR spectrum (red solid, first panel), sum of the simulated signals (black dashed, first panel), and individual simulated signals (black) of the products of reaction 22. Signals are present at g=1.97, $A(^{139}\text{La})=153.4~\text{G}~([\text{La}^{\text{II}}\text{Cp'}_3]^{\text{I-}},$ second panel), $g_A=1.96$, $A_A(^{139}\text{La})=186.5~\text{G}~(\text{La-A}, \text{third panel})$, and $g_B=1.96$, $A_B(^{139}\text{La})=229.8~\text{G}~(\text{La-B}, \text{fourth panel})$.

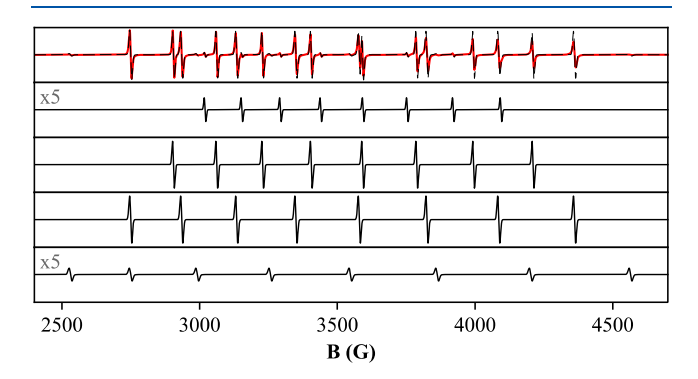


Figure 6. Room-temperature X-band EPR spectrum (red solid, first panel), sum of the simulated signals (black dashed, first panel), and individual simulated signals (black) of the products of reaction 23. Signals are present at g=1.97, $A=153.5~\mathrm{G}~([\mathrm{La^{II}Cp'_3}]^{1-}$, second panel, magnified \times 5), $g_A=1.96$, $A_A(^{139}\mathrm{La})=186.4~\mathrm{G}~(\mathrm{La-A}$, third panel), $g_B=1.96$, $A_B(^{139}\mathrm{La})=230.0~\mathrm{G}~(\mathrm{La-B}$, fourth panel), and g=1.96, $A(^{139}\mathrm{La})=290.0~\mathrm{G}~([\mathrm{La^{II}Cp^{tet}_3}]^{1-}$, fifth panel, magnified \times 5).

experiment. Ligand exchange is well-known in Ln(III) chemistry. Support for this assessment comes from the EPR spectrum of $[Y^{II}Cp''_{2}Cp]^{1-}$ ($g=1.99, A(^{89}Y)=34.6$ G), which differs from both that of " $[Y^{II}Cp''_{3}]^{1-}$ " ($g=1.99, A(^{89}Y)=36.1$ G) and that of " $[Y^{II}Cp_{3}]^{1-}$ " ($g=1.99, A(^{89}Y)=42.8$ G). [La $^{II}Cp''_{3}]^{1-}$ + KA (A = Anionic Ligand): Ligand

[La^{II}Cp"₃]¹⁻ + KA (A = Anionic Ligand): Ligand Exchange Reactions. To investigate whether ligand exchange could be the cause of these extra signals (i.e., La-A, La-B, La-C, and La-D) in addition to those of the known compounds, reactions of [La^{II}Cp"₃]¹⁻ with potassium salts were examined. Experiments were carried out with La(II) since its eight-line

patterns are easier to simulate and are less prone to obfuscation by other signals, as is the case with the two-line patterns of Y(II). [La^{II}Cp"₃]¹⁻ was treated with KCp' to determine whether this would lead to ligand exchange with the La(II) complex (reaction 26). The EPR spectrum of the product mixture contains four La(II) signals: those of the known [La^{II}Cp'₃]¹⁻ (g=1.97, $A(^{139}La)=153.4$ G) and [Cp"₃La^{II}]¹⁻ (g=1.97, $A(^{139}La)=134$ G) as well as those of La-C ($g_C=1.97$, $A_C(^{139}La)=144.6$ G) and La-D ($g_D=1.97$, $A_D(^{139}La)=149.7$ G) from reaction 25 (Figure 7). This result supports the hypothesis that these extra species

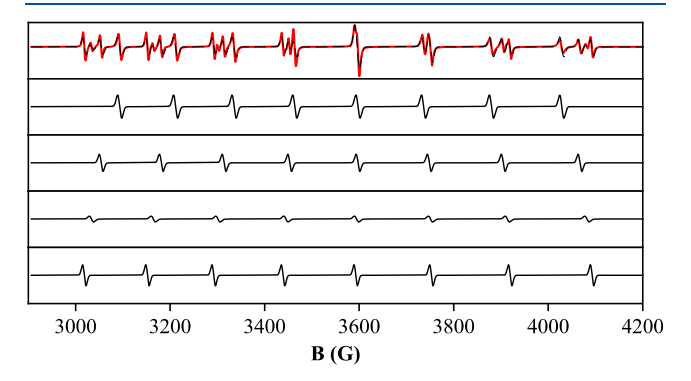


Figure 7. Room-temperature X-band EPR spectrum (red solid, first panel), sum of the simulated signals (black dashed, first panel), and individual simulated signals (black) of the products of reaction 26. Signals are present at g=1.97, $A(^{139}\text{La})=133.6$ G ([La $^{\text{II}}\text{Cp'}_3$] $^{\text{I}}$ -, second panel), $g_{\text{C}}=1.97$, $A_{\text{C}}(^{139}\text{La})=144.6$ G (La-C, third panel), $g_{\text{D}}=1.97$, $A_{\text{D}}(^{139}\text{La})=149.7$ G (La-D, fourth panel), and g=1.97, $A(^{139}\text{La})=153.4$ G ([La $^{\text{II}}\text{Cp'}_3$] $^{\text{I}}$ -, fifth panel).

observed in the EPR spectra are the result of ligand exchange. Hence, both alkali metal salts (reaction 26) and La(III) compounds (reaction 25) can act as Cp' ligand transfer agents. Furthermore, if all of the EPR-detectable La(II) compounds in reaction 26 are assumed to be tris(cyclopentadienyl) compounds (N.B., this is not necessarily true, as $[K(crypt)][La^{III}Cp'_4]$ is known),²⁸ there is a maximum of four unique species, corresponding to the number of species seen in reaction 26: $[La^{II}Cp''_3]^{1-}$, $[La^{II}Cp''_2Cp']^{1-}$, $[La^{II}Cp''Cp'_2]^{1-}$, and $[La^{II}Cp''_3]^{1-}$. The results of reactions 22, 23, 25, and 26 are shown in Table 1.

$$[La^{II}Cp''_{3}]^{1-} + 3KCp' \rightarrow [La^{II}Cp''_{3}]^{1-} + [La^{II}Cp'_{3}]^{1-} + La-C + La-D$$
 (26)

Since the signals for the putative heteroleptic La(II) compounds also occur in reaction 25, ligand exchange experiments between La^{III}Cp''_3 and La^{III}Cp'_3(THF) were carried out in THF- d_8 and C_6D_6 to investigate by NMR

Table 1. Simulated Room-Temperature X-Band EPR Parameters of Reactions of La Complexes

assignment	rxn 22	rxn 23	rxn 25	reverse of rxn 25	rxn 26
$[La^{II}Cp''_3]^{1-}$			133.6 (367.3), 1.96	133.5 (367.2), 1.96	133.6 (367.8), 1.97
La-C			144.8 (398.0), 1.96	144.8 (398.0), 1.96	144.6 (398.0), 1.97
La-D			149.8 (411.9), 1.96	149.7 (411.8), 1.97	149.7 (412.2), 1.97
$[La^{II}Cp'_{3}]^{1-}$	153.4 (422.5), 1.97	153.4 (422.3), 1.97			153.4 (422.5), 1.97
La-A	186.5 (512.5), 1.96	186.3 (512.1), 1.96			
La-B	229.8 (630.5), 1.96	230.0 (631.0), 1.96			
$[La^{II}Cp^{tet}_{3}]^{1-}$		290.0 (794.1), 1.96			

[&]quot;Assignments were made on the basis of published EPR parameters. 1,4,14 Spectra were simulated using EasySpin. 29 Values are the $A(^{139}La)$ value in Gauss (MHz), followed by the g value.

spectroscopy whether ligand exchange occurs in the La(III) state. New Cp" and Cp' environments were observed at room temperature (in the THF- d_8 experiment, one new environment each for Cp" and Cp'; in the C₆D₆ experiment, two new environments each for Cp" and Cp') that were distinct from La^{III}Cp"₃, La^{III}Cp'₃(THF), KCp", and KCp' (Figures S39 and S40, respectively). When the THF- d_8 solution was reduced using KC₈ both in the presence and in the absence of crypt, La-C and La-D were observed.

Early attempts to synthesize $[La^{II}Cp''_3]^{1-}$ by reduction of $La^{II}Cp''_3$ in dimethoxyethane (DME) led to the isolation of $[La^{III}Cp''_2(\mu\text{-}OMe)]_2$ via cleavage of OMe groups from DME, presumably by $[La^{II}Cp''_3]^{1-}$ 30. The reported EPR spectrum of a DME solution of $[La^{II}Cp''_3]^{1-}$ at 295 K shows multiple species: one that was assigned to $[La^{II}Cp''_3]^{1-}$ ($g=1.97, A(^{139}La)=134.1$ G), which was eventually isolated, and another that was suggested to arise from $La^{II}Cp''_2(DME)_x$ ($g=1.97, A(^{139}La)=145.1$ G). This second species was never crystallographically authenticated. It seems possible that the second EPR signal could arise from a heteroleptic " $[La^{II}Cp''_2(OMe)]^{1-}$ " complex formed by reduction of the $[La^{III}Cp''_2(\mu\text{-}OMe)]_2$ decomposition product of this reaction. The reaction of KOMe with $[La^{II}Cp''_3]^{1-}$ was examined to determine whether such a complex could be accessed by ligand exchange. The EPR spectrum of reaction 27 indicates the presence of two La(II) species: one assignable to $[La^{II}Cp''_3]^{1-}$ ($g=1.97, A(^{139}La)=133.6$ G) and another species that is a near match for the second species seen in the spectrum of $[La^{II}Cp''_3]^{1-}$ in DME ($g=1.96, A(^{139}La)=144.8$ G).

$$[La^{II}Cp''_{3}]^{1-} + 3KOMe \rightarrow [La^{II}Cp''_{3}]^{1-} + other La(II)$$

$$species \tag{27}$$

[Ln^{II}A₃]¹⁻ versus Traditional Ln(II) Compounds. The reducing capacities of the traditional Ln(II) ions Sm(II), Tm(II), Dy(II), and Nd(II) to make the new Ln(II) ions of La and Y were also investigated. This offered a chance to bracket the electrochemical potentials more precisely since a few complexes of the traditional ions have already been electrochemically characterized. Reactions between the Sm(II) compounds Sm^{II}2(THF)₅, Sm^{II}(C₅Me₅)₂(THF)₂, Sm^{II}(C₅Me₅)₂, and Sm^{II}Cp''₂(THF)³⁶ and the trivalent lanthanide complexes La^{III}Cp''₃ and Y^{III}Cp'₃ did not yield any La(II) or Y(II) products. Hence, Sm(II) is less reducing than any of the new La(II) or Y(II) ions. Eu(II) and Yb(II) complexes were not investigated, as they are known to be weaker reductants than Sm(II). TmI₂(DME)₃, TDyI₂, and NdI₂. also failed to reduce either La^{III}Cp''₃ or Y^{III}Cp'₃ to La(II) or Y(II) products, respectively, at -35 °C in THF.

DISCUSSION

Since the redox couple for $[La^{III/II}Cp''_3]^{0/1-}$ has been measured at $-2.8~V~vs~Fc^+/Fc~(THF, 0.2~M~[NBu_4][PF_6])$, 30 it is possible to rank the reduction potentials of other complexes relative to this couple using the results of this study. $[La^{II}Cp^{tet}_3]^{1-}$ and $[La^{II}Cp'_3]^{1-}$ are stronger reductants than $[La^{II}Cp''_3]^{1-}$, so the reduction potentials of their corresponding La(III) complexes are more negative than $-2.8~V~vs~Fc^+/Fc$. Since the potentials of $[Ln^{II}Cp'_3]^{1-}$ (Ln=Y,Lu) are similar to that of $[La^{II}Cp'_3]^{1-}$, the corresponding Ln(III) complexes can also be estimated to have reduction potentials more negative than $-2.8~V~vs~Fc^+/Fc$. Since $[Y^{II}(NR_2)_3]^{1-}$ and $[Y^{II}(OAr)_3]^{1-}$ are stronger reductants than

 $[Y^{II}Cp'_{3}]^{1-}$, the amide and aryloxide compounds also have reduction potentials more negative than $-2.8 \text{ V vs Fc}^+/\text{Fc}$.

The finding that $[La^{II}Cp''_3]^{I-}$ is the weakest reductant studied here may explain the fact that the reduction of $La^{III}Cp''_3$ can be carried out under N_2 without formation of an $(N_2)^{2-}$ complex. In contrast, reductions of $La^{III}(Cp^{tet})_3$ and $La^{III}(C_5Me_5)_2(BPh_4)$ complexes under N_2 all form reduced dinitrogen complexes containing $[La^{III}_2(\mu-\eta^2:\eta^2-N_2)]^{4+}$ moieties. It may be the case that La(II) complexes of Cp'' do not have enough reducing capacity to activate N_2 in this fashion. This is consistent with ligand choice for Ln(II) complexes being an important parameter in determining small-molecule activation chemistry.

This study shows that NR_2 and OAr ligands give complexes that are stronger reductants than Cp' for Y. This roughly follows the trend of the hyperfine coupling constant values observed in the EPR spectra of the $[Y^{II}A_3]^{1-}$ complexes, i.e., A = OAr (156 G), NR_2 (110 G), and Cp' (36.6 G). Similarly, the La studies show that Cp^{tet} and Cp' are more reducing than Cp'', following the trend of the A values for the $[La^{II}A_3]^{1-}$ complexes, i.e., $A = Cp^{tet}$ (291 G), Cp' (154 G), and Cp'' (133 G). Interestingly, this study shows that the relative reducing capacity of one metal versus another depends on the ligand. For example, Y(II) is more reducing than Gd(II) with Cp' ligands, whereas the reverse is true with NR_2 ligands.

In the course of this study, EPR signals for complexes beyond the known $[La^{II}A_3]^{1-}$ and $[Y^{II}A_3]^{1-}$ complexes were observed that are consistent with the presence of numerous heteroleptic Ln(II) complexes. Ligand exchange is common in the chemistry of trivalent lanthanide complexes and evidently can also occur with $4d^1$ Y(II) and $5d^1$ La(II). Reactions 25 and 26 clearly show that ligand exchange can occur between Ln(II) compounds and Ln(III) or alkali metal compounds as ligand transfer agents.

Lastly, the findings from reaction 27 suggest that the first report 30 of $[La^{II}Cp''_{3}]^{1-}$ also reported the first EPR spectrum of " $[La^{II}Cp''_{2}(OMe)]^{1-}$ ", since the parameters observed in that report nearly match those seen for reaction 27. While " $[La^{II}Cp''_{2}(OMe)]^{1-}$ " has not been crystallographically authenticated here and a hyperfine coupling constant is not a unique identifier of a compound, this is a plausible explanation and speaks to the diversity of Ln(II) compounds possible in heteroleptic ligand environments as well as the power of EPR spectroscopy to detect them.

CONCLUSIONS

Electron transfer and ligand exchange in Ln(II) compounds were observed using EPR spectroscopy. In compounds [Ln^{II}Cp'₃]¹⁻, the ordering of metals from most reducing to least reducing is $Tb(II) \gtrsim Y(II) \approx La(II) \approx Lu(II) > Gd(II)$. In compounds $[Ln^{II}(NR_2)_3]^{1-}$, the order is $Tb(II) \approx Gd(II) \gtrsim$ Y(II) > Sc(II), with Gd(II) becoming a stronger reductant than Y(II) by a change of ligand set. When [Ln^{II}A₃]¹⁻ compounds are compared by changing the identity of the anion (A), no clear rule determines which ligand sets are more or less reducing, but a loose correlation between the magnitude of the hyperfine coupling constant in the EPR spectrum and strong reducing ability is noted. Extensive ligand exchange is seen alongside electron transfer in these experiments. The observation of these ligand exchange products in the EPR spectra suggests that many heteroleptic Ln(II) compounds are accessible and await the development of targeted syntheses and full characterization.

■ EXPERIMENTAL SECTION

All manipulations and syntheses were conducted with the rigorous exclusion of air and water using standard Schlenk line and glovebox techniques under an argon atmosphere. Solvents were sparged with ultrahigh-purity argon and dried by passage through columns containing Q-5 and molecular sieves prior to use. Deuterated NMR solvents were dried over NaK alloy or Na/benzophenone, degassed by three freeze-pump-thaw cycles, and vacuum-transferred before use. ¹H NMR spectra were recorded on a Bruker AVANCE 600 spectrometer (¹H operating at 600 MHz) at 298 K, unless otherwise stated, and referenced internally to residual protio-solvent resonances. EPR spectra were collected using X-band frequencies (9.3-9.8 GHz) on a Bruker EMX spectrometer equipped with an ER4119HS-W1 microwave bridge, and the magnetic field was calibrated with DPPH (g = 2.0036). Compounds $Ln^{III}Cp'_{3}(THF)_{x}$ (Ln = Y_{2}^{2} La,³⁹ Gd,⁴ Tb, = 2.0036). Compounds Ln Cp $_3(I \Pi r)_x (L\Pi - 1, La, Gu, Ic, Lu)^{39} x = 1$ for Ln = La, x = 0 for Y, Gd, Tb, Lu), Ln $^{III}(NR_2)_3 (Ln = Sc, Ic, Lu)$ Lu; x = 1 for Lh = La, x = 0 for I, Gd, 1b, Lu), Lh (NR_2)₃ (Lh = Sc, Y, Gd, Tb), 40 $Y^{III}(OAr)_3$, 41 $Sc^{III}(OAr')_3$, 13 $La^{III}Cp^{tet}_3$, 42 $La^{III}Cp^{r'}_3$, 43 KCp', 39 $Sm^{II}_2(THF)_5$, 33 $Sm^{II}(C_5Me_5)_2(THF)_2$, 34 $Sm^{II}(C_5Me_5)_2$, 35 $Sm^{II}Cp''_2(THF)$, 36 Dy^{II}_2 , 22 Nd^{II}_2 , and KC_8 , 44 were synthesized by published preparations. KOMe was synthesized by reacting potassium metal with a THF solution of an excess of MeOH (based on potassium) overnight and then removing solvent in vacuo and washing the resulting white solids with hexane and diethyl ether. EPR parameters for $[Ln^{II}Cp'_3]^{1-}(Ln=Y,^2La,^4Gd,^4Lu^4), [Ln^{II}(NR_2)_3]^{1-}(Ln=Sc,^6Y^{26}), [Y^{II}(OAr)_3]^{1-,13} [Sc^{II}(OAr')_3]^{1-,13} [La^{II}Cp^{tet}_3]^{1-,14}$ and $[La^{II}Cp''_3]^{1-}$ were taken from literature reports. In the initial report of $[K(crypt)][La^{II}Cp''_3]$, the EPR spectroscopic parameters were reported to be g=1.990 and $A(^{139}La)=133.5$ G.¹ In all of the simulations in this work, reactions where $[La^{II}Cp^{\prime\prime}{}_{3}]^{1-}$ is present (as either a reactant or a product), it was best modeled as having g = 1.96and $A(^{139}La) = 133.5$ G. All of the EPR parameters were taken from simulations of the room-temperature spectra using EasySpin. 25

ASSOCIATED CONTENT

Supporting Information

The Supporting Information is available free of charge at https://pubs.acs.org/doi/10.1021/acs.organomet.9b00837.

EPR and NMR spectra (PDF)

AUTHOR INFORMATION

Corresponding Author

William J. Evans — Department of Chemistry, University of California, Irvine, California 92697-2025, United States; orcid.org/0000-0002-0651-418X; Email: wevans@uci.edu

Author

Samuel A. Moehring — Department of Chemistry, University of California, Irvine, California 92697-2025, United States;
o orcid.org/0000-0002-6619-7737

Complete contact information is available at: https://pubs.acs.org/10.1021/acs.organomet.9b00837

Notes

The authors declare no competing financial interest.

ACKNOWLEDGMENTS

We thank the U.S. National Science Foundation for support of this research under CHE-1855328. We also thank Professor A. S. Borovik, Dr. Ethan A. Hill, Dr. Victoria F. Oswald, and Justin L. Lee for their generous assistance with EPR spectroscopy, Professor A. F. Heyduk for helpful conversations, and Dr. Nicholas R. Rightmire, Tener F. Jenkins, Austin J. Ryan, Daniel N. Huh, Jessica R. K. White, and Sierra R. Ciccone for providing compounds for analysis.

REFERENCES

- (1) Hitchcock, P. B.; Lappert, M. F.; Maron, L.; Protchenko, A. V. Lanthanum Does Form Stable Molecular Compounds in the +2 Oxidation State. *Angew. Chem., Int. Ed.* **2008**, 47, 1488–1491.
- (2) MacDonald, M. R.; Ziller, J. W.; Evans, W. J. Synthesis of a Crystalline Molecular Complex of Y²⁺, [(18-crown-6)K]-[(C₅H₄SiMe₃)₃Y]. J. Am. Chem. Soc. **2011**, 133, 15914–15917.
- (3) MacDonald, M. R.; Bates, J. E.; Fieser, M. E.; Ziller, J. W.; Furche, F.; Evans, W. J. Expanding rare-earth oxidation state chemistry to molecular complexes of holmium(II) and erbium(II). *J. Am. Chem. Soc.* **2012**, *134*, 8420–8423.
- (4) MacDonald, M. R.; Bates, J. E.; Ziller, J. W.; Furche, F.; Evans, W. J. Completing the Series of +2 Ions for the Lanthanide Elements: Synthesis of Molecular Complexes of Pr²⁺, Gd²⁺, Tb²⁺, and Lu²⁺. *J. Am. Chem. Soc.* **2013**, *135*, 9857–9868.
- (5) Fieser, M. E.; MacDonald, M. R.; Krull, B. T.; Bates, J. E.; Ziller, J. W.; Furche, F.; Evans, W. J. Structural, Spectroscopic, and Theoretical Comparison of Traditional vs Recently Discovered Ln^{2+} Ions in the $[K(2.2.2\text{-cryptand})][(C_5H_4SiMe_3)_3Ln]$ Complexes: The Variable Nature of Dy^{2+} and Nd^{2+} . J. Am. Chem. Soc. **2015**, 137, 369–382.
- (6) Woen, D. H.; Chen, G. P.; Ziller, J. W.; Boyle, T. J.; Furche, F.; Evans, W. J. Solution Synthesis, Structure, and CO₂ Reduction Reactivity of a Scandium(II) Complex, {Sc[N(SiMe₃)₂]₃} -. Angew. Chem., Int. Ed. 2017, 56 (8), 2050–2053.
- (7) Evans, W. J. Tutorial on the role of cyclopentadienyl ligands in the discovery of molecular complexes of the rare-earth and actinide metals in new oxidation states. *Organometallics* **2016**, *35*, 3088–3100.
- (8) Woen, D. H.; Evans, W. J. Expanding the +2 Oxidation State of the Rare-Earth Metals, Uranium, and Thorium in Molecular Complexes. In *Handbook on the Physics and Chemistry of Rare Earths*; Elsevier, 2016; Vol. 50, pp 337–394.
- (9) Gould, C. A.; McClain, K. R.; Yu, J. M.; Groshens, T. J.; Furche, F.; Harvey, B. G.; Long, J. R. Synthesis and Magnetism of Neutral, Linear Metallocene Complexes of Terbium(II) and Dysprosium(II). *J. Am. Chem. Soc.* **2019**, *141*, 12967–12973.
- (10) Kelly, R. P.; Maron, L.; Scopelliti, R.; Mazzanti, M. Reduction of a Cerium(III) Siloxide Complex To Afford a Quadruple-Decker Arene-Bridged Cerium(II) Sandwich. *Angew. Chem., Int. Ed.* **2017**, *56*, 15663—15666.
- (11) Fieser, M. E.; Palumbo, C. T.; La Pierre, H. S.; Halter, D. P.; Voora, V. K.; Ziller, J. W.; Furche, F.; Meyer, K.; Evans, W. J. Comparisons of lanthanide/actinide +2 ions in a tris(aryloxide)arene coordination environment. *Chem. Sci.* **2017**, *8*, 7424–7433.
- (12) Ryan, A. J.; Darago, L. E.; Balasubramani, S. G.; Chen, G. P.; Ziller, J. W.; Furche, F.; Long, J. R.; Evans, W. J. Synthesis, Structure, and Magnetism of Tris(amide) {Ln[N(SiMe₃)₂]₃}¹ Complexes of the Non-Traditional +2 Lanthanide Ions. *Chem. Eur. J.* **2018**, 24, 7702–7709.
- (13) Moehring, S. A.; Beltrán-Leiva, M. J.; Páez-Hernández, D.; Arratia-Pérez, R.; Ziller, J. W.; Evans, W. J. Rare-Earth Metal(II) Aryloxides: Structure, Synthesis, and EPR Spectroscopy of [K(2.2.2-cryptand)][Sc($OC_6H_2tBu_2$ -2,6-Me-4) $_3$]. Chem. Eur. J. 2018, 24, 18059—18067.
- (14) Jenkins, T. F.; Woen, D. H.; Mohanam, L. N.; Ziller, J. W.; Furche, F.; Evans, W. J. Tetramethylcyclopentadienyl Ligands Allow Isolation of Ln(II) Ions across the Lanthanide Series in [K(2.2.2-cryptand)][($C_5Me_4H)_3Ln$] Complexes. *Organometallics* **2018**, 37, 3863–3873.
- (15) Angadol, M. A.; Woen, D. H.; Windorff, C. J.; Ziller, J. W.; Evans, W. J. Tert-Butyl(cyclopentadienyl) Ligands Will Stabilize Nontraditional +2 Rare-Earth Metal Ions. *Organometallics* **2019**, *38* (5), 1151–1158
- (16) Huh, D. N.; Ziller, J. W.; Evans, W. J. Isolation of reactive Ln(ii) complexes with C5H4Me ligands (CpMe) using inverse sandwich countercations: synthesis and structure of [(18-crown-6)K(μ -CpMe)-K(18-crown-6)][CpMe₃Ln^{II}] (Ln = Tb, Ho). Dalton Trans **2018**, 47 (48), 17285–17290.
- (17) Woen, D. H.; Huh, D. N.; Ziller, J. W.; Evans, W. J. Reactivity of Ln(II) Complexes Supported by $(C_5H_4Me)^-$ Ligands with THF and

- PhSiH₃: Isolation of Ring-Opened, Bridging Alkoxyalkyl, Hydride, and Silyl Products. *Organometallics* **2018**, *37*, 3055–3063.
- (18) Electrochemical Series. In CRC Handbook of Chemistry and Physics, 100th ed. (Internet Version 2019); Rumble, J. R., Ed.; CRC Press/Taylor & Francis: Boca Raton, FL, 2019.
- (19) Arnold, P. L.; Cloke, F. G. N.; Nixon, J. F. The first stable scandocene: synthesis and characterisation of bis(η -2,4,5-tri-tert-butyl-1,3-diphosphacyclopentadienyl)scandium(II). *Chem. Commun.* **1998**, 797–798.
- (20) Huang, R. H.; Faber, M. K.; Moeggenborg, K. J.; Ward, D. L.; Dye, J. L. Structure of K⁺(cryptand[2.2.2]) electride and evidence for trapped electron pairs. *Nature* **1988**, *331*, 599–601.
- (21) Dye, J. L. Electrides: Ionic salts with electrons as the anions. *Science* **1990**, 247 (4943), 663–668.
- (22) Bochkarev, M. N.; Fagin, A. A. A new route to neodymium(II) and dysprosium(II) iodides. *Chem. Eur. J.* **1999**, *5* (10), 2990–2992.
- (23) Evans, W. J.; Drummond, D. K.; Zhang, H.; Atwood, J. L. Synthesis and X-ray Crystal Structure of the Divalent [Bis-(trimethylsilyl)amido]samarium Complexes [(Me₃Si)₂N]₂Sm(THF)₂ and {[(Me₃Si)₂N]Sm(μ -I) (DME) (THF)}₂. Inorg. Chem. **1988**, 27 (3), 575–579.
- (24) Tilley, T. D.; Andersen, R. A.; Zalkin, A. Divalent Lanthanide Chemistry. Preparation and Crystal Structures of Sodium Tris[bis-(trimethylsilyl)amido]europate(II) and Sodium Tris[bis-(trimethylsilyl)amido]ytterbate(II), NaM[N(SiMe₃)₂]₃. *Inorg. Chem.* 1984, 23, 2271–2276.
- (25) Ryan, A. J.; Ziller, J. W.; Evans, W. J. The Importance of the Counter-cation in Reductive Rare-Earth Metal Chemistry: 18-Crown-6 Instead of 2,2,2-Cryptand Allows Isolation of [Y^{II}(NR₂)₃]¹⁻ and Ynediolate and Enediolate Complexes from CO Reactions. *Chem. Sci.* **2020**, *11*, 2006–2014.
- (26) Fang, M.; Lee, D. S.; Ziller, J. W.; Doedens, R. J.; Bates, J. E.; Furche, F.; Evans, W. J. Synthesis of the $(N_2)^{3-}$ Radical from Y^{2+} and Its Protonolysis Reactivity To Form $(N_2H_2)^{2-}$ via the $Y[N(SiMe_3)_2]_3/KC_8$ Reduction System. J. Am. Chem. Soc. **2011**, 133, 3784–3787.
- (27) Corbey, J. F.; Woen, D. H.; Palumbo, C. T.; Fieser, M. E.; Ziller, J. W.; Furche, F.; Evans, W. J. Ligand Effects in the Synthesis of Ln²⁺ Complexes by Reduction of Tris(cyclopentadienyl) Precursors Including C—H Bond Activation of an Indenyl Anion. *Organometallics* **2015**, *34*, 3909–3921.
- (28) Kotyk, C. M.; Macdonald, M. R.; Ziller, J. W.; Evans, W. J. Reactivity of the Ln^{2+} Complexes [K(2.2.2-cryptand)]- $[(C_5H_4\operatorname{SiMe}_3)_3\operatorname{Ln}]$: Reduction of Naphthalene and Biphenyl. *Organometallics* **2015**, 34, 2287–2295.
- (29) Stoll, S.; Schweiger, A. EasySpin, a comprehensive software package for spectral simulation and analysis in EPR. *J. Magn. Reson.* **2006**, *178*, 42–55.
- (30) Cristina Cassani, M.; Lappert, M. F.; Laschi, F. First identification by EPR spectra of lanthanum(II) organometallic intermediates (and $E_{1/2}$ for $La^{3+} \rightarrow La^{2+}$) in the C–O bond activation of dimethoxyethane. *Chem. Commun.* **1997**, 1563–1564.
- (31) Finke, R. G.; Keenan, S. R.; Schiraldi, D. A.; Watson, P. L. Organolanthanide and Organoactinide Oxidative Additions Exhibiting Enhanced Reactivity. 3. Products and Stoichiometries for the Addition of Alkyl and Aryl Halides to $(C_5Me_5)_2Yb^{II} \bullet OEt_2$ and Evidence for Facile, Inner-Sphere $(C_5Me_5)_2Yb^{III}R$ and $(C_5Me_5)_2Yb^{III}X$. Organometallics 1986, 5, 598–601.
- (32) Anderson, L. B.; Macero, D. J. The formal reduction potential of the europium(III)-europium(II) system. *J. Phys. Chem.* **1963**, *67*, 1942.
- (33) Evans, W. J.; Gummersheimer, T. S.; Ziller, J. W. Coordination Chemistry of Samarium Diiodide with Ethers Including the Crystal Structure of Tetrahydrofuran-Solvated Samarium Diiodide, SmI₂(THF)₅. J. Am. Chem. Soc. **1995**, 117, 8999–9002.
- (34) Evans, W. J.; Hunter, W. E.; Grate, J. W.; Choi, H. W.; Bloom, I.; Atwood, J. L. Solution Synthesis and Crystallographic Characterization of the Divalent Organosamarium Complexes $(C_5Me_5)_2Sm(THF)_2$ and $[(C_5Me_5)Sm(\mu\text{-I})(THF)_2]_2$. J. Am. Chem. Soc. **1985**, 107, 941–946.
- (35) Evans, W. J.; Hughes, L. A.; Hanusa, T. P. Synthesis and Crystallographic Characterization of an Unsolvated, Monomeric

- Bis(pentamethylcyclopentadienyl) Organolanthanide Complex, (C₅Me₅)₂Sm. *J. Am. Chem. Soc.* **1984**, 106, 4270–4272.
- (36) Evans, W. J.; Keyer, R. A.; Ziller, W. Synthesis and reactivity of bis(trimethylsilyl)cyclopentadienyl samarium complexes including the X-ray crystal structure of $[(Me_3Si)_2C_5H_3]_3Sm$. *J. Organomet. Chem.* **1990**, 394, 87–97.
- (37) Bochkarev, M. N.; Fedushkin, I. L.; Fagin, A. A.; Petrovskaya, T. V.; Ziller, J. W.; Broomhall-Dillard, R. N. R.; Evans, W. J. Synthesis and Structure of the First Molecular Thulium (II) Complex: [TmI₂(MeOCH₂CH₂OMe)₃]. *Angew. Chem., Int. Ed. Engl.* 1997, 36, 133–135.
- (38) Evans, W. J.; Lee, D. S.; Lie, C.; Ziller, J. W. Expanding the LnZ₃ /Alkali-Metal Reduction System to Organometallic and Heteroleptic Precursors: Formation of Dinitrogen Derivatives of Lanthanum. *Angew. Chem., Int. Ed.* **2004**, *43*, 5517–5519.
- (39) Peterson, J. K.; MacDonald, M. R.; Ziller, J. W.; Evans, W. J. Synthetic Aspects of $(C_5H_4SiMe_3)_3Ln$ Rare-Earth Chemistry: Formation of $(C_5H_4SiMe_3)_3Lu$ via $[(C_5H_4SiMe_3)_2Ln]^+$ Metallocene Precursors. Organometallics 2013, 32, 2625–2631.
- (40) Bradley, D. C.; Ghotra, J. S.; Hart, F. A. Low Co-ordination Numbers in Lanthanide and Actinide Compounds. Part 1. The Preparation and Characterization of Tris{bis(trimethylsilyl)-amido)-lanthanides. *J. Chem. Soc., Dalton Trans.* 1973, 1021–1023.
- (41) Steele, L. A. M.; Boyle, T. J.; Kemp, R. A.; Moore, C. The selective insertion of carbon dioxide into a lanthanide(III) 2,6-dit-butyl-phenoxide bond. *Polyhedron* **2012**, 42 (1), 258–264.
- (42) Schumann, H.; Glanz, M.; Hemling, H.; Hahn, F. E. Metallorganische Verbindungen der Lanthanoide. 93. Tetramethylcyclopentadienyl-Komplexe ausgewählter 4f-Elemente. Z. Anorg. Allg. Chem. 1995, 621, 341–345.
- (43) Laschi, F.; Hitchcock, P. B.; Gun'ko, Y. K.; Cassani, M. C.; Lappert, M. F. Synthesis and Characterization of Organolanthanidocene(III) (Ln = La, Ce, Pr, Nd) Complexes Containing the 1,4-Cyclohexa-2,5-dienyl Ligand (Benzene 1,4-Dianion): Structures of $[K([18]\text{-crown-6})][Ln\{\eta^5-C_5H_3(\text{SiMe}_3)_2-1,3\}_2(C_6H_6)][Cp''=\eta^5-C_5H_3(\text{SiMe}_3)_2-1,3$; Ln. Organometallics 1999, 18, 5539–5547.
- (44) Bergbreiter, D. E.; Killough, J. M. Reactions of Potassium-Graphite. J. Am. Chem. Soc. 1978, 100 (7), 2126-2134.